

A novel assist-steering method with direct yaw moment for distributed-drive articulated heavy vehicle

Tao Xu¹ , Xuewu Ji¹ and Yanhua Shen²

Abstract

This paper presents a novel assist-steering method for distributed-drive articulated heavy vehicles (DAHVs) to reduce its dependency on hydraulic steering method and improve the pressure characteristics of hydraulic struts. The objective is to realise the electrification of steering process for DAHVs, which is the basis of unmanned design with more stable control in the following studies. The theory and purpose of the proposed assist-steering method in this paper distinguishes it from the traditional direct yaw-moment control method or assist-steering methods in the previous studies, which easily produce interference with hydraulic steering method in DAHVs during steering process. In this paper, an accurate vehicle model is developed along with the field test for its satisfactory verification. Meanwhile, with the decoupling analyses of two different effects of steering methods on vehicle steering process, the assist-steering method is developed. In order to show the advantages brought on by this method, a case study is performed and analyzed. The results demonstrate that this proposed method can reduce the pressure of hydraulic steering system to about 41.2% without any changes of steering process, which is limited by the drive ability of wheel-side motor. Moreover, the pressure of inlet chamber in hydraulic struts is always reduced to about 40%–60% without any changes of the pressure in outlet chamber, which can improve the working performance of hydraulic steering system.

Keywords

Assist-steering method, hydraulic steering method, direct yaw moment, distributed-drive articulated heavy vehicle

Date received: 31 July 2019; accepted: 14 October 2019

Introduction

Articulated heavy vehicles (AHVs), the particular mechanism in engineering, are widely used in the mining, forest and construction industry. Its structure consists of front and rear parts, connected by an articulation joint and two hydraulic struts. With the coupling effects of these two units, the vehicle can be turned under the driven of hydraulic steering system. It follows the control of steering wheel, which is called as hydraulic steering method.^{1–3} Otherwise, when each of the wheels of AHVs is equipped with wheel-side motor independently, it is named as distributed-drive articulated heavy vehicles (DAHVs). DAHVs have better performance than AHVs in maneuverability and stability, which have aroused much research interest, especially for its steering process.^{4–7}

Nowadays, owing to the greater steering resistance of DAHVs under heavy loads, the higher pressure in hydraulic steering system is required, which causes the structural redundancy, the strict sealing condition, and more energy consumption in hydraulic

steering system during the steering process.^{8,9} Although optimizing the vehicle structure can reduce the hydraulic pressure, the resulting improvements are limited because of the load characteristics of DAHVs.⁹ Meanwhile, due to the compressible characteristic of hydraulic oil and the special structure of DAHVs, the steering process cannot keep stable and is easy to cause snaking behavior, especially in the unmanned process.^{4,10} Therefore, this paper presents an assist-steering method with appropriate direct yaw moment for DAHVs, which is used to reduce the pressure requirements of the hydraulic steering system and

¹State Key Laboratory of Automotive Safety and Energy, Tsinghua University, Beijing, China

²School of Mechanical Engineering, University of Science and Technology Beijing, Beijing, China

Corresponding author:

Tao Xu, State Key Laboratory of Automotive Safety and Energy, Tsinghua University, Haidian, Beijing 10084, China.
Email: ustb_xt@163.com

Proc IMechE Part K:
J Multi-body Dynamics
2020, Vol. 234(1) 214–224
© IMechE 2019
Article reuse guidelines:
sagepub.com/journals-permissions
DOI: 10.1177/1464419319889531
journals.sagepub.com/home/pik



improve its working condition of hydraulic struts during steering process.

The direct yaw moment is usually produced by the differential driving/braking forces of wheels, which is easily realised in the vehicle with motor-driven wheels.^{7,10–14} In several studies, this direct yaw moment is generally used to improve the vehicle stability. Azad et al.⁷ controlled the left- and right-wheels of the vehicle to produce the direct yaw moment to prevent the oscillatory instability of an articulated steer vehicle. They evaluated the performance of the controller by conducting several simulations based on a linearized model, which was verified in ADAMS. Başlamoğlu et al.¹⁰ proposed an integrated active front steering and differential control method for the vehicle to improve its handling stability. Cherouat and Diop¹² presented a controller with the braking/traction forces to improve the vehicle dynamics performance and stability. Asiabar and Kazemi¹³ presented a direct yaw moment controller for four wheel-side motor drive electric vehicle to improve the vehicle handling and yaw stability. These studies make the direct yaw moment generated by driving/braking wheel forces that apply into the vehicle for its stability, which is much different with the assist-steering methods proposed for DAHVs in this paper.

Besides, there was still a literature that used the direct yaw moment to assist the vehicle in steering. Iida et al.¹⁵ applied a direct yaw moment controller into an AHV to improve its steering performance. Experiments and simulations showed that direct yaw-moment generated by one-sided braking forces during steering process can decrease the turning radius of the vehicle. Generally, when the direct yaw moment is implemented to assist the vehicle to steer, it is named as skid steering or differential steering. Skid steering is widely used in tracked vehicles, skid-steer loaders, all-terrain vehicles, and industrial robots.^{16–19} Its control methods are mostly based on the steering theory of tracked vehicles. But, compared to DAHVs, its structure and steering process are much different. Consequently, the properties of assist-steering methods with direct yaw moment for DAHVs must be studied anew combining with the characteristics of hydraulic steering process.

The aim of this paper is to provide an effective assist-steering method with direct yaw moment for DAHVs. The controller is designed with the decoupling analyses of steering process considering two different steering methods. The proposed assist-steering method reduces the dependence of DAHVs on hydraulic steering system greatly and improves the working condition of hydraulic struts. In addition, it is different with existing study in previous researches. This method uses the differential driving forces of all wheels to generate the direct yaw moment, which can guarantee the accuracy of assist-steering moment whether in the transient or stability steering process.

Modelling of DAHVs

Vehicle modelling

The motions of DAHVs are realised with the coupling effect of hydraulic struts and articulation joint. It transfers the forces between front and rear parts of the vehicle. When the DAHVs move on the straight line, these two components are locked. But during the steering process, they are relaxed, and permit the two parts of the vehicle to rotate relatively. This movement can be divided into two steps: (1) The struts are driven by pump. In turn, they push the two parts of the vehicle to steer and change the articulation angle; (2) With the certain articulation angle at every moment, the vehicle is driven to steer. This motion process follows the principle of least resistance, which is explained in Xu et al.²⁰ Different from the dynamic analyses in ‘Case study’ section of Xu et al.²⁰, the completed dynamic vehicle model considering the longitude, lateral, and yaw effects on front and rear parts is developed in this research to discuss the force characteristics during steering process. The schematic diagram of the vehicle model is shown in Figure 1.

In Figure 1, a global coordinate system $O(x, y, z)$ is created with its origin located at the articulation point. The positive direction of x -axis is toward the front part of the vehicle, the positive direction of y -axis is perpendicular to the vehicle longitudinal direction and toward the right side, and the z -axis is perpendicular to the ground. $O_f(x_f, y_f, z_f)$ and $O_r(x_r, y_r, z_r)$ are the coordinate system with the origin point located at the mass center of the front and rear parts and moving with the vehicle. L is the wheel track. a and b are the distances between the front and rear wheel axle and articulation joint, respectively. L_{f0} and L_{r0} are the distances from the mass center to the axles of front and rear parts, respectively. F_{hRf} , F_{hRr} , F_{hLf} and F_{hLr} are the forces of hydraulic struts acting on the different parts of the

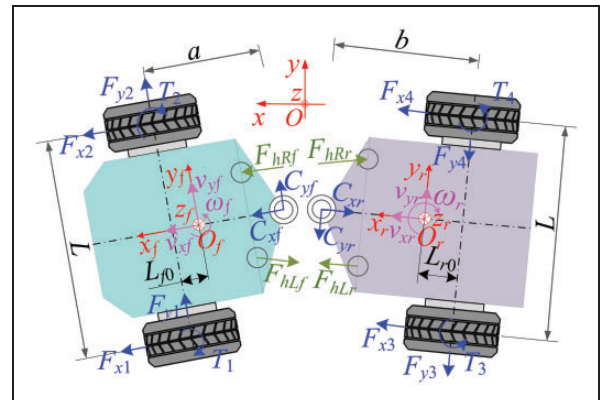


Figure 1. Schematic of DAHVs model. DAHV: distributed-drive articulated heavy vehicle.

vehicle. v_{xf} , v_{yf} and ω_f represent the velocity along the longitudinal, lateral and yawing direction for the front part of the vehicle, which are the same as the meaning of v_{xr} , v_{yr} and ω_r for the rear part. C_{xf} , C_{yf} , C_{xr} and C_{yr} are the forces at the articulation joint in front and rear parts of the vehicle, respectively. F_{xi} and F_{yi} ($i=1-4$) represent the longitudinal and lateral tyre forces of the i th wheel where i is the front-left, front-right, rear-left, or rear-right wheel. T_i is the aligning torque of the i th wheel.^{6,21,22}

The dynamic model of DAHVs considering the longitudinal, lateral, and yaw motions can be expressed by

$$\begin{cases} m_f(\dot{v}_{xf} + v_{yf} \cdot \omega_f) = C_{xf} + F_{hx} + F_{wx} \\ m_f(\dot{v}_{yf} - v_{xf} \cdot \omega_f) = C_{yf} + F_{hy} + F_{wy} \\ I_z \dot{\omega}_f = -(T_1 + T_2) + T_{Cyzf} + T_{hz} + T_{wyzf} + T_{wxzf} \\ m_r(\dot{v}_{xr} - v_{yr} \cdot \omega_r) = -C_{xr} + F_{hx} + F_{wx} \\ m_r(\dot{v}_{yr} + \omega_r v_{xr}) = -C_{yr} + F_{hy} + F_{wy} \\ -I_{zr} \dot{\omega}_r = T_3 + T_4 + T_{Cyzr} + T_{hzr} + T_{wyzr} + T_{wxzr} \end{cases} \quad (1)$$

where m_f and m_r are the masses of front and rear parts of the vehicle, respectively. F_{hx} and F_{hy} are the forces of the hydraulic struts along the x -axis and y -axis of the coordinate system, respectively. F_{wx} and F_{wy} are the wheel forces along the same direction as F_{hx} and F_{hy} , respectively. I_z is the mass moment of inertia. T_{wyz} , T_{wxz} , T_{hz} , and T_{Cyz} are the moments around the z_f -axis coordinate system, which are produced by the wheels, hydraulic struts, and articulation joint, respectively. These parameters can be obtained as follows.

1. The forces of hydraulic struts acted on the front part are

$$\begin{cases} F_{hx} = -F_{hLf} \cdot \cos(\theta_{fL}) + F_{hRf} \cos(\theta_{fR}) \\ F_{hy} = F_{hLf} \cdot \sin(\theta_{fL}) - F_{hRf} \sin(\theta_{fR}) \end{cases} \quad (2)$$

where θ_{fL} and θ_{fR} are the angles between the front part of the vehicle and the left or right hydraulic struts.²⁰ F_{hLf} and F_{hRf} are the forces of the left and right hydraulic struts, respectively. It can be expressed as

$$\begin{cases} F_{hLf} = P_{in} A_p - P_{out} A_a \\ F_{hRf} = P_{in} A_a - P_{out} A_p \end{cases} \quad (3)$$

where A_p and A_a represent the effective piston area and annular area of the rod-side chamber in hydraulic strut, respectively. P_{in} is the pressure in piston-side chamber of right strut or rod-side chamber of left strut, while P_{out} is the pressure in piston-side chamber of left strut or rod-side chamber of right strut. As for

these two parameters, P_{in} is unknown which are the outputs of this vehicle model, and P_{out} can be obtained from the analyses of 'Appendix' section.²⁰

2. The tyre forces along the x -axis and y -axis are given as

$$\begin{cases} F_{wx} = F_{x1} + F_{x2} \\ F_{wy} = F_{y1} + F_{y2} \end{cases} \quad (4)$$

where F_{x1} and F_{x2} represent the longitudinal tyre forces, while F_{y1} and F_{y2} are the lateral tyre forces. In this research, the linear tyre model is chosen to calculate these forces, which can be expressed by

$$\begin{cases} F_x = \begin{cases} \zeta_f s_i & i = 1, 2 \\ \zeta_r s_i & i = 3, 4 \end{cases} \\ F_y = \begin{cases} k_f \alpha_i & i = 1, 2 \\ k_r \alpha_i & i = 3, 4 \end{cases} \end{cases} \quad (5)$$

where ζ_f and ζ_r are the driving coefficient of tyre in front and rear parts of the vehicle, respectively. s is the slip rate of tyre. k_f and k_r are the cornering stiffness of tyre in front and rear parts of the vehicle, respectively. α is the side-slip angle of tyre.

3. The moment around the z_f -axis produced by the articulation joint is given as

$$T_{Cyzf} = C_{yf} \cdot (a - L_{f0}) \quad (6)$$

4. The moment around the z_f -axis produced by the two hydraulic struts is given as

$$\begin{aligned} T_{yzf} = & F_{hLf} \cdot \cos(\theta_{fL}) \cdot L_{fL} + F_{hRf} \cdot \cos(\theta_{fR}) \cdot L_{fR} \\ & + \dots + (F_{hLf} \cdot \sin(\theta_{fL}) - F_{hRf} \cdot \sin(\theta_{fR})) \\ & \cdot (a - L_{f0} - a_f) \end{aligned} \quad (7)$$

where L_{fL} , L_{fR} are the distances from the centerline of the vehicle frame to the conjunction point of hydraulic struts.²⁰

5. The moments around z_f -axis produced by the wheels are given as

$$\begin{cases} T_{wxzf} = (-F_{x1} + F_{x2}) \cdot \frac{L}{2} \\ T_{wyzf} = -(F_{y1} + F_{y2}) \cdot L_{f0} \end{cases} \quad (8)$$

The dynamic behavior of the rear part of the DAHVs can refer to equations (2) to (8).

Combined with the analyses of vehicle movements, the motion relationship between front and rear part

can be derived as

$$\begin{cases} v_{xr} = v_{xf} \cos(\theta) + (v_{yf} + \omega_f \cdot (a - L_{f0})) \sin(\theta) \\ v_{yr} = -v_{xf} \sin(\theta) + (v_{yf} + \omega_f \cdot (a - L_{f0})) \cos(\theta) - \dots \\ -\omega_r(a - L_{r0}) \end{cases} \quad (9)$$

where θ is the articulation angle of the vehicle.

With the analyses above, the angular velocities of front and rear parts of the vehicle consist of two motion process: the movement because of the struts and the movement because of the constant articulation angle with velocity. Combining equation (10) with Xu et al.,²⁰ the angular velocities of front and rear parts are shown as

$$\begin{cases} \omega_f = \omega_v + \dot{\theta}_f \\ \omega_r = -\omega_v + \dot{\theta}_r \end{cases} \quad (10)$$

where ω_v is the angular velocity of the vehicle with constant articulation angle and a certain velocity. It is the same parameter for the front and rear parts of the vehicle that should be solved from dynamic analysis of this section. ω_f and ω_r are the yaw rate of the front and rear parts of the vehicle, respectively. These two parameters are the superposition of two different parts of steering process that have been introduced above. θ_f and θ_r are the articulation angle of front and rear parts of the vehicle.²⁰

By solving the derivative of equations (9) and (10), the accelerations of the rear part of DAHVs can be expressed as

$$\begin{cases} \left\{ \begin{array}{l} \dot{v}_{xr} = \dot{v}_{xf} \cos(\theta) + (\dot{v}_{yf} + \dot{\omega}_f \cdot L_f) \sin(\theta) \\ -\dot{\theta}(v_{xf} \sin(\theta) - (v_{yf} + \omega_f \cdot L_f) \cos(\theta)) \end{array} \right\} \\ \left\{ \begin{array}{l} \dot{v}_{yr} = -\dot{v}_{xf} \sin(\theta) + (\dot{v}_{yf} + \dot{\omega}_f \cdot L_f) \cos(\theta) \\ -\dot{\omega}_r L_r - \dot{\theta}(v_{xf} \cos(\theta) + (v_{yf} + \omega_f \cdot L_f) \sin(\theta)) \end{array} \right\} \\ \ddot{\omega}_r = \ddot{\theta}_f + \ddot{\theta}_r - \dot{\omega}_f \end{cases} \quad (11)$$

where L_f and L_r are the distances from the mass centre to the articulation joint, $L_f = a - L_{f0}$, $L_r = b - L_{r0}$, respectively.

The forces on the articulation joint of rear part can be derived by the forces on the front part

$$\begin{cases} C_{xr} = C_{xf} \cdot \cos(\theta) + C_{yf} \cdot \sin(\theta) \\ C_{yr} = -C_{yf} \cdot \sin(\theta) + C_{xf} \cdot \cos(\theta) \end{cases} \quad (12)$$

Combining equations (2) to (12) and the dynamic analyses for the rear part of the vehicle, equation (1) can be rewritten as

$$R\dot{X} = H + G \begin{bmatrix} P_{in} \\ P_{out} \end{bmatrix} + G' \quad (13)$$

where R and H are shown by equations (22) and (23) in Appendix 1, respectively. X , G and G' can be expressed by equations (14) and (15)

$$X = [v_{xf} \ v_{yf} \ \omega_{zf} \ \omega_{zr}]^T \quad (14)$$

$$\begin{cases} G = \begin{bmatrix} a_{11} & a_{12} & a_{13} & a_{14} & a_{15} & a_{16} \\ a_{21} & a_{22} & a_{23} & a_{24} & a_{25} & a_{26} \end{bmatrix} \\ G' = \begin{bmatrix} a_{31} & a_{32} & a_{33} & a_{34} & a_{35} & a_{36} \end{bmatrix} \end{cases} \quad (15)$$

where $a_{11} - a_{36}$ are shown by equation (24) in Appendix 1.

Otherwise, a speed controller (PID controller) is also designed to keep the longitudinal velocity of the vehicle in this model. It follows the control of drivers, and its output is required for drive torque T_d . Generally, most of the DAHVs distribute the drive torque equally. Its output drive torque is T_r . And in this research, the influence of motor controller is ignored, considering the limitation of the drive ability (T_{max}) of each wheel-side motor only. The whole framework of this vehicle model is shown in Figure 2.

In Figure 2, φ is the steering wheel angle. Y_L and Y_R are the lengths of hydraulic struts.²⁰ v_{ref} is the required vehicle velocity controlled by the driver. v_{xf} is the velocity of front part of the vehicle. T_{ti} is the drive torque of each wheel-side motor.

Field test and verification

Field tests are performed with a loaded 35t DAHV. The experimental area is shown in Figure 3. The parameters of vehicle and hydraulic steering system, and the input of the vehicle model are shown in Xu et al.²⁰ With these parameters, the mathematical model in MATLAB/Simulink is implemented. The response comparison of the simulation with measure data is shown in Figure 4.

The description of Figure 4(a) to (d) has been introduced in Xu et al.²⁰ Figure 4(e) represents the pressure in rod-side chamber of right strut and piston-side chamber of left strut, and Figure 4(f) represents the pressure in piston-side chamber of right strut and rod-side chamber of left strut. The maximum error of pressure is about 1 MPa, which is related with the precision of sensors.

According to the agreements of these simulations and measured data, the negligible error could validate that the theory and steering model described above are accurate compared to the real steering process of DAHVs. This model can be used to study the intelligent control for DAHVs.

Researches on assist-steering method for DAHVs

Based on the introduction above, DAHVs are equipped with wheel-side motors. Its wheels are

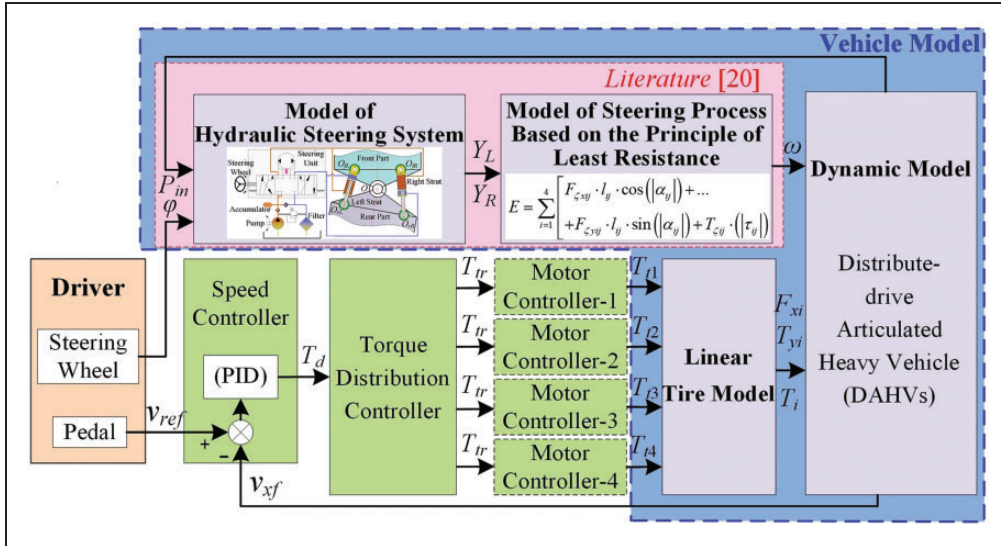


Figure 2. Framework of vehicle model.

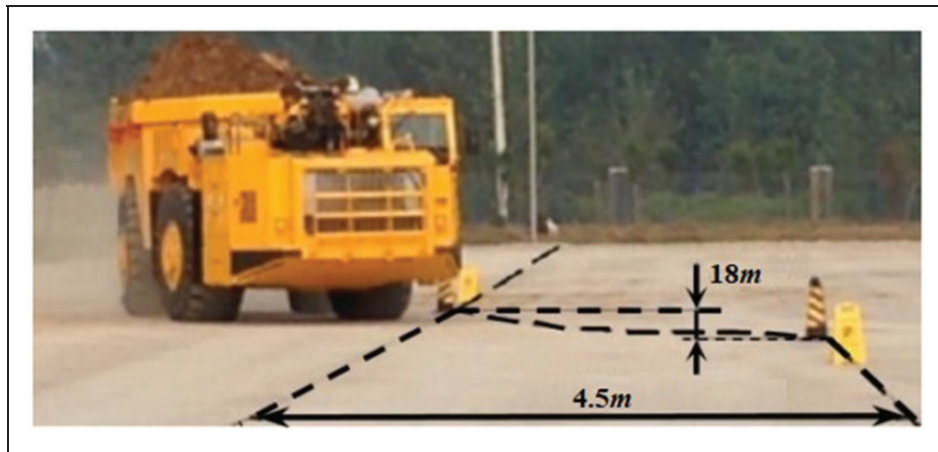


Figure 3. The experimental area of field test.

controlled independently. When the motor drive wheels with different driving force in the left and right side, the additional yaw-moment (direct yaw moment) can be produced and influences the motion of the vehicle. According to equation (13), the vehicle dynamic equation is shown by

$$R\dot{X}_e = H + G \begin{bmatrix} P_{in} \\ P_{out} \end{bmatrix} + G' + \dots + [\Delta T_{df}r, 0, \Delta M_f, \Delta T_{dr}r, 0, \Delta M_r]^T \quad (16)$$

where X_e is the vehicle dynamic parameters with the influence of direct yaw moment. ΔT_{df} and ΔT_{dr} are the additional drive torque in front and rear parts of the vehicle, which are used to reduce the influence of additional yaw moment on the vehicle velocity. r is the effective radius of tyre. ΔM_f and ΔM_r are the direct yaw moment of front and rear parts of the vehicle.

Equation (16) shows the coupling effect of the hydraulic steering method and assist-steering method

on the vehicle steering process. With the decoupling analysis of equation (16), it can be rewritten by

$$\begin{aligned} \dot{X}_e &= \underbrace{(KD + K')G \begin{bmatrix} P_{in} \\ P_{out} \end{bmatrix}}_{\dot{X}_{eh}} + H' \\ &\quad + \underbrace{(KD + K')[\Delta T_{df}r, 0, \Delta M_f, \Delta T_{dr}r, 0, \Delta M_r]^T}_{\dot{X}_{ed}} \end{aligned} \quad (17)$$

where X_{eh} is the effect of hydraulic steering method on vehicle steering process, while X_{ed} is the influence of direct yaw moment. H' , K and K' are the constant matrix, which can be expressed by equations (18) to (20). The constant matrix D is shown by equation (25) in Appendix 1.

$$H' = KDG' + K'G' \quad (18)$$

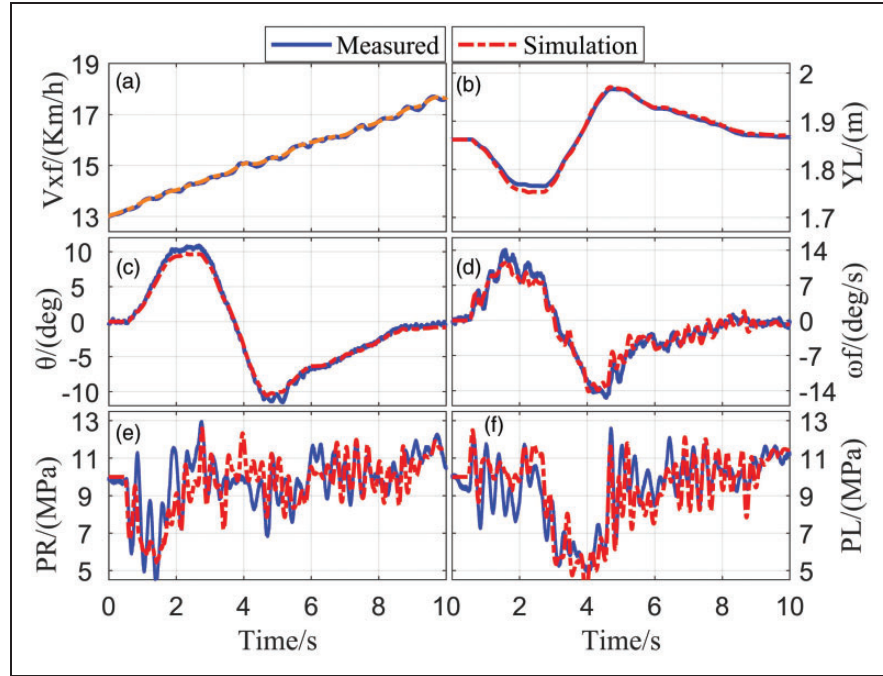


Figure 4. Response comparison of simulation results with measure data. (a) velocity of the vehicle; (b) length of left hydraulic strut; (c) articulation angle of the vehicle; (d) yaw rate of vehicle front part; (e) pressure in piston-side chamber of right hydraulic strut; (f) pressure in piston-side chamber left hydraulic strut.

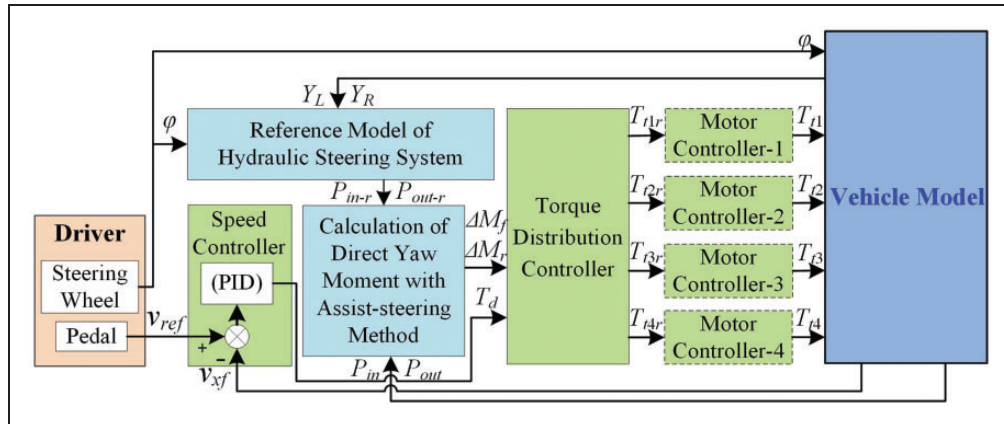


Figure 5. Framework of assist-steering method for DAHVs. DAHV: distributed-drive articulated heavy vehicle.

$$K = \begin{bmatrix} K_{11} & K_{12} & K_{13} \\ K_{21} & K_{22} & K_{23} \\ K_{31} & K_{32} & K_{33} \\ K_{41} & K_{42} & K_{43} \end{bmatrix} \quad (19)$$

$$K' = \begin{bmatrix} \frac{1}{m_1} & 0 & 0 & 0 & 0 & 0 \\ 0 & \frac{1}{m_1} & 0 & 0 & 0 & 0 \\ 0 & 0 & \frac{1}{I_z} & 0 & 0 & 0 \\ 0 & 0 & 0 & 0 & 0 & 0 \end{bmatrix} \quad (20)$$

where K_{11} – K_{43} are the constants, which are represented by equation (26) in Appendix 1.

Equation (17) shows two different effects of steering method on vehicle steering process. If the direct yaw moment is implemented on the vehicle, its dynamic characteristic must be changed. Otherwise, when the effect of hydraulic steering method is reduced actively (such as reducing the pressure of accumulator, which influence the pressure of hydraulic struts directly), the appropriate additional yaw moment can be obtained from equation (17) to keep the vehicle in reasonable steering process. Correspondingly, the vehicle can reduce the dependency of the steering process on the hydraulic steering method, which is the principle of assist-steering method in this paper. However, as there is no relatively reasonable motion process for DAHVs, the assist-steering method in this research

Table 1. The parameters of DAHV.

Description	Symbol	Unit	Value
Maximum torque	T_{emax}	Nm	2577
Tyre effective radius	R	Mm	1032

DAHV: distributed-drive articulated heavy vehicle.

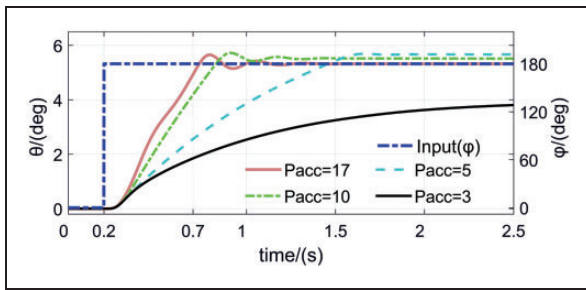


Figure 6. Steering process without assist-steering method.

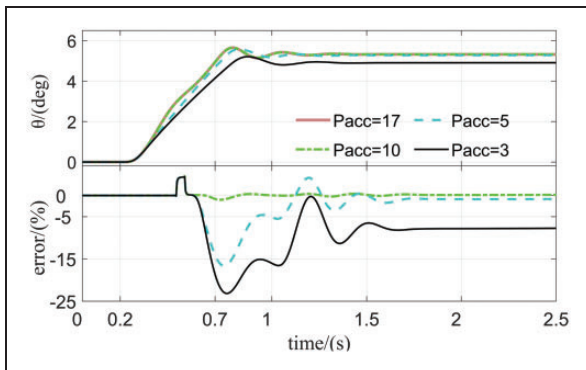


Figure 7. Steering process with assist-steering method.

can make the vehicle follow the original hydraulic steering process, and the use of pressure hydraulic strut obtained from the model of hydraulic steering system can be used as the reference. The general framework is shown in Figure 5.

In Figure 5, T_{tr} is the required torque of each wheel-side motor under the influence of direct yaw moment. It can be represented by

$$\begin{cases} T_{t1r} = T_{\text{tr}} - \frac{\Delta M_f}{L} + \frac{\Delta T_{df}}{2} \\ T_{t2r} = T_{\text{tr}} - \frac{\Delta M_f}{L} + \frac{\Delta T_{df}}{2} \\ T_{t3r} = T_{\text{tr}} - \frac{\Delta M_r}{L} + \frac{\Delta T_{dr}}{2} \\ T_{t4r} = T_{\text{tr}} - \frac{\Delta M_r}{L} + \frac{\Delta T_{dr}}{2} \end{cases} \quad (21)$$

Case study

In this section, 35t DAHV that has been used in the field test is implemented to develop the simulation and verify the assist-steering method introduced above. The parameters of this vehicle are explained in Xu et al.²⁰ The other related vehicle parameters are shown in Table 1.

The main principle of the assist-steering method is by reducing the steering force of hydraulic steering system actively and making the direct yaw moment to supply the insufficient steering force. But due to the limitation of drive ability of each wheel-side motor, the driving force used to steer the vehicle may be insufficient to keep the normal steering process. Figures 6 and 7 show the vehicle steering process without and with assist-steering method under step inputs of steering wheel angle (The maximum steering wheel angle is 180°, the vehicle velocity is kept at 20 km/h, and on the concrete road). There is no special standard for the verification of steer angle

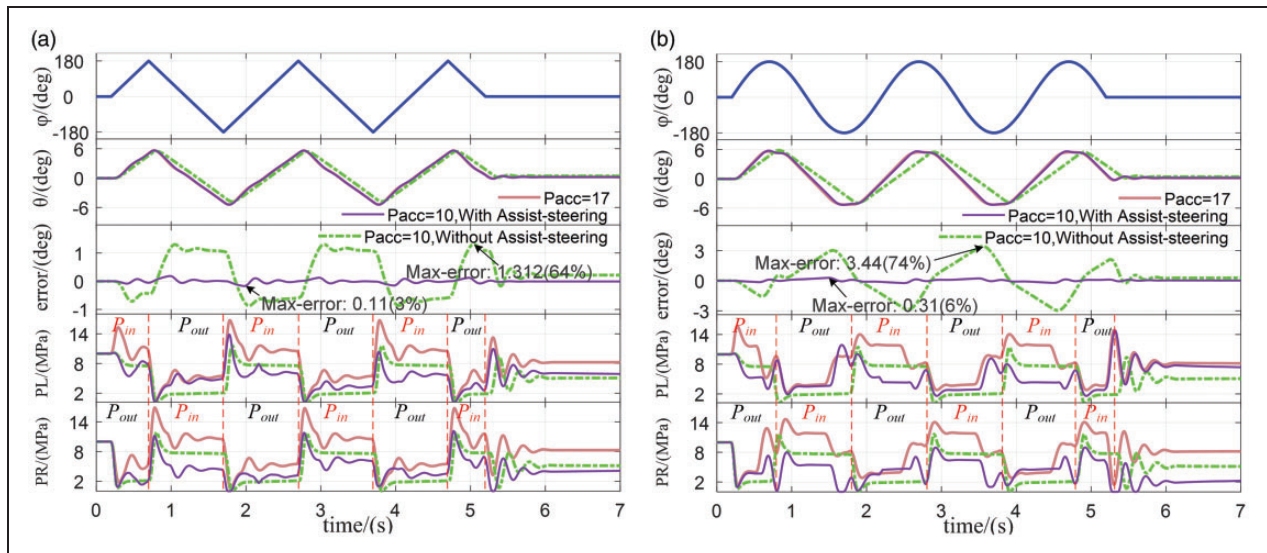


Figure 8. Steering process of DAHVs with assist-steering method under different inputs of steering wheel angle. (a) Triangular wave input of steering wheel angle. (b) Sine wave input of steering wheel angle. DAHV: distributed-drive articulated heavy vehicle.

manoeuvre of DAHVs. The step-inputs of steering wheel angle follow the standard of traditional passenger cars (“GB-T 6323-2014/Controllability and stability test procedure for automobile” in China).

In these two figures, P_{acc} is the pressure of accumulator, which represents the drive pressure of hydraulic steering system. Its original value is 17 MPa in test vehicle. According to the simulation result in Figure 6, the understeering of the vehicle will appear along with the reduction of P_{acc} . When the direct yaw moment is implemented during the steering process, the understeering of the vehicle can be reduced, which is shown in Figure 7. But the improvement of the vehicle steering performance is limited due to the drive ability of each wheel-side motor. Based on these analyses, this paper chose 10 MPa as the pressure of accumulator (reduce the pressure about 41.2%), although there is about 1% error compared with the original vehicle steering process. Under these chosen parameters, the simulation is implemented with different input (the continuous Sine-input and impulse-input) of steering wheel angle to verify the vehicle steering process with assist-steering method. The inputs of the simulation follow the standard of GB-T 6323-2014 (in China). In these two simulations, the driver accelerated the vehicle to 20 km/h, and turns the vehicle to the left at 0.2 s for about 0.5 s. Then the vehicle is turned back to the right side at 0.7 s for about 1 s, and so on. In these simulations, the maximum steering wheel angle is 180°, and the vehicle is on the smooth concrete road. The inputs and the simulation results are shown in Figure 8.

It can be seen from Figure 8 that when the pressure of accumulator is reduced actively, no matter what kind of input of steering wheel angle is, the vehicle with assist-steering method can track the original steering process. The maximum error is about 0.11–0.31° (3%–6%), while the maximum error without assist-steering method is about 1.312–3.44° (64%–74%). Meantime, this method can reduce the pressure of inlet chamber of hydraulic steering system about 40%–60% without increasing the pressure of outlet chamber. These changes contribute to improve the sealing characteristic and reduce the energy consumption of hydraulic steering system.

Conclusion

The goal of this study was to propose a new assist-steering method for DAHVs, which was realised with the direct yaw moment produced by different driving force of each wheel. It is used to reduce the vehicle dependency on hydraulic steering method, realise the electrification during steering process, and improve its working performance.

This paper was the first one to bring the assist-steering method with direct yaw moment into

DAHVs and help the hydraulic steering system to steer. The accurate mathematical vehicle model and reasonable verification technology with field test were presented briefly combining with the pre-existing literature. Based on this model, the assist-steering method was designed. But due to the limitation of driving ability of wheel-side motor, the pressure of accumulator can only be reduced to about 41.2%, which means that this assist-steering method can partially replace the traditional hydraulic steering method during the steering process. Based on these analyses, the two different inputs of steering wheel angle are chosen to make simulation. The results demonstrated that the proposed assist-steering method was effective for DAHVs to steer and reduce its dependency on hydraulic steering method. In addition, the pressure of outlet chamber in hydraulic struts is reduced to about 40%–60% when the pressure of outlet chamber is not changed, which can greatly improve the working condition of hydraulic steering system.

As an extension of this work, the more effective assist-steering method will be introduced into DAHVs without limitation of drive ability in wheel-side motor. Meanwhile, the solenoid valve will be used to replace the hydraulic steering system completely and to realise more effective control during the steering process. Furthermore, based on this new structure, the upper controller will be designed to improve the vehicle stability.

Declaration of Conflicting Interests

The author(s) declared no potential conflicts of interest with respect to the research, authorship, and/or publication of this article.

Funding

The author(s) disclosed receipt of the following financial support for the research, authorship, and/or publication of this article: this work was supported by the National Natural Science Foundation of China (Grant No. 51875035) (China), and the China Scholarships Council (No. 201706460074).

ORCID iD

Tao Xu  <https://orcid.org/0000-0001-5889-3727>

References

1. Piotr A. Design characteristics of steering systems for mobile wheeled earthmoving equipment. *J Terramech* 1989; 26: 25–82.
2. Horton D and Crolla D. Theoretical analysis of the steering behaviour of articulated frame steer vehicles. *Vehicle Syst Dyn* 1986; 15: 211–234.
3. He Y, Khajepour A, McPhee J, et al. Dynamic modelling and stability analysis of articulated frame steer vehicles. *Int J Heavy Veh Syst* 2005; 12: 28–59.
4. Gao Y, Shen Y, Xu T, et al. Oscillatory yaw motion control for hydraulic power steering articulated vehicles considering the influence of varying bulk modulus. *IEEE Trans Contr Syst Technol* 2018; 27: 1284–1292.

5. Xu T, Shen Y and Zhang W. In-situ steering dynamics analysis of skid steering for articulated motor-driven vehicle. *SAE Int J Passenger Cars Mech Syst* 2016; 9: 903–911.
6. Yin Y, Rakheja S, Yang J, et al. Effect of articulated frame steering on the transient yaw responses of the vehicle. *Proc IMechE, Part D: J Automatic Engineering* 2018; 232: 384–399.
7. Azad N, Khajepour A and McPhee J. Robust state feedback stabilization of articulated steer vehicles. *Vehicle Syst Dyn* 2007; 45: 249–275.
8. Crolla D. *The steering behaviour of articulated body steer vehicles*. Pasadena: Road Vehicle Handling (I Mech E Conference Publications), 1983, p. 5.
9. Thulasiraman B, Arumugam G and Sadali N, et al. Steering linkage optimization of articulated construction equipment. In: *Proceedings of the 1st international and 16th national conference on machines and mechanisms*, India, 18–20 December 2013.
10. Başlamişlı SÇ, Köse IE and Anlaç G. Handling stability improvement through robust active front steering and active differential control. *Vehicle Syst Dyn* 2011; 49: 657–683.
11. Goodarzi A and Ghajar M. Integrating lane-keeping system with direct yaw moment control tasks in a novel driver assistance system. *Proc IMechE, Part K: J Multi-body Dynamics* 2015; 229: 16–38.
12. Cherouat H and Diop S. An observer and an integrated braking/traction and steering control for a cornering vehicle. *Am Control Conf* 2005; 2213: 2212–2217.
13. Asiabar A and Kazemi R. A direct yaw moment controller for a four in-wheel motor drive electric vehicle using adaptive sliding mode control. *Proceedings of the Proc IMechE, Part K: J Multi-body Dynamics* 2019; 233: 549–567.
14. Abe M. Vehicle dynamics and control for improving handling and active safety: from four-wheel steering to direct yaw moment control. *Proc IMechE, Part K: J Multi-body Dynamics* 1999; 15: 1952–1967.
15. Iida M, Nakashima H and Tomiyama H. Small-radius turning performance of an articulated vehicle by direct yaw moment control. *Comput Electron Agr* 2011; 76: 277–283.
16. Wang T, Wu Y, Liang J, et al. Analysis and experimental kinematics of a skid-steering wheeled robot based on a laser scanner sensor. *Sensors* 2015; 15: 9681–9702.
17. Fauroux J and Vaslin P. Modeling, experimenting, and improving skid steering on a 6×6 all-terrain mobile platform. *J Field Robot* 2010; 27: 107–126.
18. Janarthanan B, Padmanabhan C and Sujatha C. Lateral dynamics of single unit skid-steered tracked vehicle. *Int J Auto Tech* 2011; 12: 865–875.
19. Ni J, Hu J and Li X. Dynamic modelling, validation and handling performance analysis of a skid-steered vehicle. *Proc IMechE, Part D: J Automatic Engineering* 2016; 230: 514–526.
20. Xu T, Shen Y, Huang Y, et al. Study of hydraulic steering process for articulated heavy vehicle based on the principle of the least resistance. *IEEE/ASME T Mech* 2019; 24: 1662–1673.
21. Zhuang J. *The vehicle tire*. Beijing: Beijing Institute of Technology Press, 1995.
22. Wong J. *Theory of ground vehicles*. New York: John Wiley & Sons, Inc, 2008.

Appendix

Notation

A	the distance between front wheel axle and articulation joint
A_a	effective annular area of the rod-side chamber in hydraulic strut
A_p	effective piston area of hydraulic strut
b	the distance between rear wheel axle and articulation joint
C_x	longitudinal forces of articulation joint
C_y	lateral forces of articulation joint
F_h	the forces of hydraulic strut acting on the different parts of the vehicle
F_w	force of the vehicle produced by tyres
F_x	longitudinal forces of tyre
F_y	lateral forces of tyre
I_z	mass moment of inertia
K	cornering stiffness of tyre
L	wheel track
L_{f0}	distance from mass center to axles of front parts
m	vehicle mass
P_{acc}	pressure of accumulator
P_{in}	pressure in piston-side chamber of right strut or rod-side chamber of left strut
P_{out}	pressure in piston-side chamber of left strut or rod-side chamber of right strut
r	effective tyre radius
s	slip rate of tyre
T	aligning torque of tyre
T_{Cyz}	the moment of the vehicle produced by articulation joint
T_d	required drive torque of the vehicle
T_{emax}	maximum torque of wheel-side motor
T_{hz}	drive torque of the vehicle produced by hydraulic strut
T_t	drive torque of each wheel-side motor
T_{tr}	required torque of each wheel-side motor
T_{wxz}	drive torque of the vehicle produced by longitudinal forces of tyres
T_{wyz}	drive torque of the vehicle produced by lateral forces of tyres
v_{ref}	required vehicle velocity
v_x	longitudinal vehicle velocity
v_y	lateral vehicle velocity
Y	the length of hydraulic strut
α	side-slip angle of tyre
θ	articulation angle of the vehicle
θ_{fL}	the angle between front part of the vehicle and left hydraulic strut
θ_{fR}	the angles between front part of the vehicle and right hydraulic strut
ω	real angular velocity of the vehicle
ω_v	angular velocity of the vehicle with constant articulation angle and a certain velocity

φ	steering wheel angle
ΔT_d	additional drive torque of the vehicle
ΔM	direct yaw moment of the vehicle
f	front part of the vehicle
r	rear part of the vehicle
R	right side of the vehicle
L	left side of the vehicle
i	($i=1\sim 4$) front-left, front-right, rear-left, or rear-right wheels
x	the x -axis of coordinate system
y	the y -axis of coordinate system
z	the z -axis of coordinate system

Appendix I

$$R = \begin{bmatrix} m_1 & 0 & 0 & 0 \\ 0 & m_1 & 0 & 0 \\ 0 & 0 & I_{zf} & 0 \\ m_2 \cos(\theta) & m_2 \sin(\theta) & m_2(a - L_{f0}) \sin(\theta) & -\cos(\theta) \\ -m_2 \sin(\theta) & m_2 \cos(\theta) & m_2 L_f \cos(\theta) & -m_2 L_r \\ 0 & 0 & 0 & -I_{zr} \end{bmatrix} \quad (22)$$

$$H = \begin{bmatrix} C_{xf} \\ C_{yf} \\ (a - L_{f0})C_{yf} \\ -\cos(\theta)C_{xf} - \sin(\theta)C_{yf} \\ \sin(\theta)C_{xf} - \cos(\theta)C_{yf} \\ -(b - L_{r0}) \sin(\theta)C_{xf} + (b - L_{r0}) \cos(\theta)C_{yf} \end{bmatrix} \quad (23)$$

$$\left\{ \begin{array}{l} a_{11} = -A_p \cos(\theta_{fL}) + A_a \cos(\theta_{fR}), a_{21} = A_a \cos(\theta_{fL}) - A_p \cos(\theta_{fR}), a_{31} = F_{wxr} - m_1 v_{yf} \omega_{zf}, \\ a_{12} = A_p \sin(\theta_{fL}) - A_a \sin(\theta_{fR}), a_{22} = -A_a \sin(\theta_{fL}) + A_p \sin(\theta_{fR}), a_{32} = F_{wyf} + m_1 v_{xf} \cdot \omega_{zf}, \\ a_{13} = A_p \cdot \cos(\theta_{fL}) \cdot L_{fL} + A_a \cdot \cos(\theta_{fR}) \cdot L_{fR} + (A_p \sin(\theta_{fL}) - A_a \sin(\theta_{fR})) (a - L_{f0} - a_f), \\ a_{23} = -A_a \cos(\theta_{fL}) \cdot L_{fL} - A_p \cos(\theta_{fR}) \cdot L_{fR} + (-A_a \sin(\theta_{fL}) + A_p \sin(\theta_{fR})) (a - L_{f0} - a_f), \\ a_{33} = -(T_1 + T_2) + T_{wyf} + T_{wxr}, a_{14} = A_p \cos(\theta_{rL}) - A_a \cos(\theta_{rR}), \\ a_{24} = -A_a \cos(\theta_{rL}) + A_p \cos(\theta_{rR}), \\ a_{34} = F_{wxr} + m_2 v_{yr} \omega_{zr} + m_2 (\omega_{zf} + \omega_{zr}) (v_{xf} \sin(\theta) - (v_{yf} + \omega_{zf} \cdot L_f) \cos(\theta)), \\ a_{15} = -A_p \sin(\theta_{rL}) + A_a \sin(\theta_{rR}), a_{25} = A_a \sin(\theta_{rL}) - A_p \sin(\theta_{rR}), \\ a_{35} = F_{wyf} - m_2 v_{xr} \omega_{zr} + m_2 (\omega_{zf} + \omega_{zr}) (v_{xf} \cos(\theta) + (v_{yf} + \omega_{zf} \cdot L_f) \sin(\theta)), \\ a_{16} = -A_p \cos(\theta_{rL}) \cdot L_{rL} - A_a \cos(\theta_{rR}) \cdot L_{rR} + (A_p \sin(\theta_{rL}) - A_a \sin(\theta_{rR})) (b - L_{r0} - b_r), \\ a_{26} = A_a \cos(\theta_{rL}) \cdot L_{rL} + A_p \cos(\theta_{rR}) \cdot L_{rR} + (-A_a \sin(\theta_{rL}) + A_p \sin(\theta_{rR})) (b - L_{r0} - b_r), \\ a_{36} = (T_3 + T_4) + T_{wyfr} + T_{wxzr} \end{array} \right. \quad (24)$$

$$D = \begin{bmatrix} \frac{m_2 \cos(\theta)}{m_1} & \frac{m_2 \sin(\theta)}{m_1} & \frac{m_2 L_f \sin(\theta)}{I_{zf}} & -1 & 0 & 0 \\ -\frac{m_2 \sin(\theta)}{m_1} & \frac{m_2 \cos(\theta)}{m_1} & \frac{m_2 L_f \cos(\theta)}{I_{zf}} & 0 & -1 & 0 \\ 0 & 0 & 0 & 0 & 0 & -1 \end{bmatrix} \quad (25)$$

$$K = \begin{bmatrix} R \frac{A_1 A_2 C_3 - A_4 A_3 C_2}{KK} & R \frac{A_1^2 C_3}{KK} & R \frac{A_1^2 C_3}{KK} \\ \frac{-(A_1 B_3 - A_3 B) A_2 + (A_1 B_2 - A_2 B) A_3}{KK} & \frac{(A_1 B_2 - A_3 B) A_1}{KK} & \frac{-(A_1 B_2 - A_2 B_1) A_1}{KK} \end{bmatrix} \quad (26)$$

where A_1-A_3 , B_1-B_3 , C_1-C_3 , KK , and U is the constant, which are shown in equation (27)

$$\begin{cases} A_1 = \left(\frac{m_2}{m_1} + 1\right) \cos(\theta), B_1 = \left(\frac{m_2}{m_1} + \frac{m_2 L_f}{I_{zf}}(a - L_{fo}) + 1\right) \sin(\theta) \\ A_2 = \left(-1 - \frac{m_2}{m_1}\right) \sin(\theta), B_2 = \left(\frac{m_2}{m_1} + \frac{m_2 L_f}{I_{zf}}(a - L_{fo}) + 1\right) \cos(\theta), C_2 = -m_2 L_r \\ A_3 = (b - L_{ro}) \sin(\theta), B_3 = -(b - L_{ro}) \cos(\theta), C_3 = -I_{zr} \end{cases} \quad (27)$$